Materials Science Forum
ISSN: 1662-9752, Vol. 1188, pp 75-83

Submitted: 2026-01-19
Revised: 2026-02-16
Accepted: 2026-02-22
Online: 2026-04-20

Digital Manufacturing of One-Off Replacement Components Using Reverse Engineering and Rapid Low-Pressure Sand Casting: Dimensional Evaluation and Key Challenges

KTARI Ahmed[1,a], LU Davis[2,b], AINSWORTH Griffin[2,c] and EL MANSORI Mohamed [1,d] *

[1]Laboratoire MSMP-EA7350, Arts et Métiers ParisTech, 2 cours des Arts et Métiers, 13617 Aix-en-Provence, France

[2]Texas A&M Engineering Experiment Station (TEES), Texas A&M university, College Station, TX, 77843, USA

[a]ahmed.ktari@ensam.eu, [b]magmagon@tamu.edu, [c]griffinainsworth@tamu.edu, [d]mohamed.elmansori@ensam.eu

Keywords: Remanufacturing by casting, Reverse engineering, 3D scanning, Sand-mold printing, 3D surface deviation

Abstract. Remanufacturing by casting of end-of-life (EoL) components can be challenging as it requires specific molds/cores, machinery and tooling. The use of 3D scanning technology and rapid casting processes can produce high-quality, efficient components. However, error propagation during the manufacturing process can significantly affect the dimensional accuracy of the final product. In this study, the dimensions of a case study part were evaluated at the main stages of the rapid hybrid low-pressure sand casting (LPSC) process, from the initial CAD model to the final casting, to identify the main causes of final 3D surface deviation. The casting design was optimized using coupled thermal and fluid-flow FE computations for two suitable casting orientations: horizontal (H) and vertical (V). After the 3D sand-mold printing process, an optical 3D scanner was used to extract surface data from each printed mold part. 3D surface deviations caused by the printing process were evaluated by comparing the individual mold components to their original CAD models using GOM Inspect Pro® software. The final castings were also compared to the initial CAD models for both orientations to quantify the overall 3D surface deviations resulting from the rapid LPSC process chain, including 3D printing, liquid metal shrinkage and contraction during solidification and cooling. The results provide a foundation for improving dimensional accuracy of one-off replacement components produced by the hybrid LPSC process.

Introduction

Remanufacturing is a key strategy in the circular economy, designed to extend product lifespans and reduce resource consumption. Its primary goal is to restore worn components or assemblies to their original or improved functional condition [1]. In recent years, remanufacturing by casting has emerged as a new branch for producing large metallic components with intricate geometries. This approach is used when direct additive manufacturing (AM) processes, typically preferred for rapid repair of localized damage, are impractical due to technical, economic, or material constraints, and when original spare parts are unavailable [2]. It enables the production of one-off replacement parts for obsolete or damaged components [3], thereby extending the service life of existing systems and supporting sustainability and resource efficiency principles.

The development of precise 3D scanning technologies, additive manufacturing, and low-pressure casting (LPC) has improved the production of one-off replacement components for complex light metal castings. The rapid LPC process reduces costs and lead times while providing better mechanical properties than traditional gravity casting [4]. However, integrating rapid LPC technology in real-world applications requires characterizing the dimensional deviations of the final casting compared to its nominal CAD. Castings without sufficient machining or heat-treating allowances are unusable, while those requiring excessive material removal by machining or grinding increase lead time and cost. It is essential to understand how dimensional errors propagate throughout the manufacturing process, from 3D scanning to final casting.

Unlike traditional sand mold casting, which requires skilled labor and time-consuming manual preparation, the AM processes accelerate the 3D sand mold production, reducing labor costs and significantly shortening production times. However, the quality of the sand mold is controlled by a number of printing parameters, including the sand grain size, the binder content, the volume of binder droplet, the recoater speed and the curing time which not only affect the mechanical properties [5], density [6] and permeability [7] of the mold but also its surface roughness [8,9] and dimensions [10–12].

Prior studies consistently show that dimensional accuracy in 3D printed sand molds (3DPSM) is influenced by both material and printing process factors. Increasing binder content or droplet diffusivity reduces dimensional accuracy due to binder bleeding and axis-dependent spreading effects, with deviations varying across the x, y, and z directions [13,14]. Build orientation also plays a significant role: vertically or 45° oriented parts exhibit better geometric fidelity than horizontally printed ones due to reduced powder compressibility [15]. This effect can be mitigated by placing parts at the bottom of the job box to improve support [12]. Additional parameters further influence shrinkage-driven deviations: finer sand grains, unfavorable grain shape, and longer curing times all increase volumetric contraction and dimensional error [16].

The use of 3D scanning technology and rapid casting processes can help produce high-quality near-net shape castings, despite the dimensional deviations that may arise from the 3D printing process of the sand mold described above. However, the dimensional deviation does not end after mold printing; it continues during the subsequent casting phase in the remanufacturing process, which can significantly affect the dimensional accuracy of the final product. This deviation can also be influenced by the casting process, as additional dimensional errors may be introduced, including mold and core expansion [17], metal shrinkage [18], core displacement [19], warping [17], and heat accumulation [20]. All these factors must be considered during the mold design stage to reduce the dimensional deviation of the remanufactured cast.

The objective of this study is to identify and analyze the key factors contributing to dimensional errors in the rapid hybrid LPSC process and to assess their impact on the dimensional deviation of parts during digital remanufacturing, from the initial CAD design to the final casting through a case study.

Materials and Methodology

In this paper, the failed part made from aluminum alloy (AlSi13Mg0.3) is scanned using Zeiss ATOS Q optical scanning technology and then processed into a 3D CAD model using Zeiss Reverse Engineering Software®. This CAD model, shown in **Fig 1**, serves as the basis for designing a sand mold.

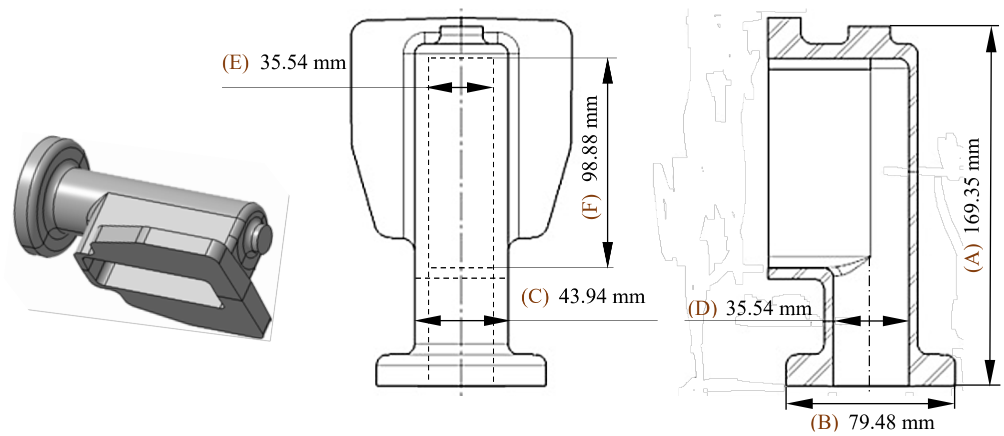

Fig. 1. The original CAD part with key characteristic dimensions

The sand mold is designed and printed according to the parameters shown in Table 1. After curing, the sand mold is brushed and cleaned to remove all loose sand particles. The 3DPSM parts were scanned and their dimensional errors compared to their original CAD were determined using Zeiss GOM Inspect Pro®. The final steps include performing the LPSC process, followed by knocking out and trimming to obtain the finished casting. The casting can then be scanned to assess the dimensional errors between the final casting and the original CAD part.

Table 1 3D printing parameters of the sand-mold

Average grain size:	140±25 μm
Resin binder content:	1.6 %
Activator content:	0.18%
Recoating speed (R_s):	0.182 m/s (14%)
X-resolution (X_r):	0.11 mm
Y-resolution (Y_r):	0.102 mm
Z-resolution (layer thickness):	0.280 mm
Print head voltage:	75 V

In addition, the dimensions of casting parts were evaluated at all stages of the rapid hybrid low-pressure sand casting (LPSC) process, from the initial CAD model to the final casting, to identify the main causes of the final 3D surface deviation. Before physical casting, each printed mold part was scanned using an optical 3D scanner. The 3D surface deviations caused by printing were determined and evaluated. The proposed methodology for evaluating the dimensional error generated in the remanufacturing process using rapid LPSC is summarized in **Fig. 2**.

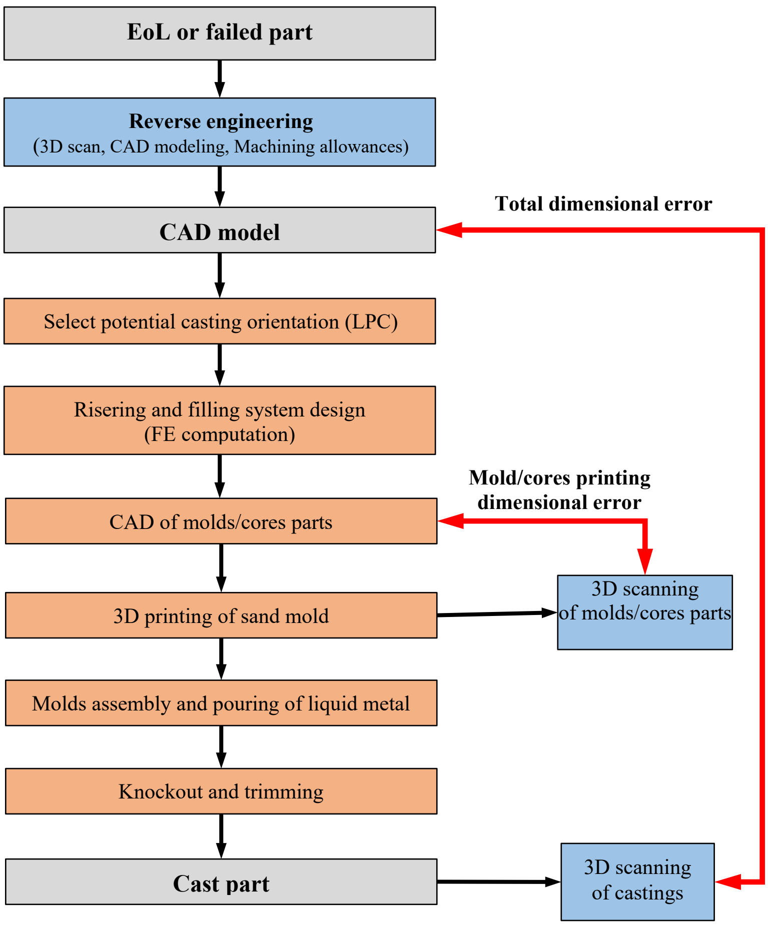

Fig. 2. Evaluation of dimensional error propagation in remanufacturing by rapid LPSC process

During remanufacturing using rapid LPSC process, dimensional errors can arise at three stages: *i)* 3D scanning of the EoL part and CAD preparation, which includes 3D scanning, CAD model reconstruction and repair, and adding casting allowances; *ii)* 3D sand mold printing and assembly; and *iii)* LPSC process. In this study, dimensional errors that occur between the original EoL part and the digitized CAD model were not considered. This decision stems from the need to apply various casting geometry repairs to the scanned EoL part to compensate for in-service phenomena such as wear, fatigue, oxidation and viscoplastic deformation. In addition, various casting allowances must be determined based on the casting material, casting process and functional surfaces. Given that the main objective of this work is tracking error propagation from the initial CAD to the final casting, only errors generated by the mold printing process and the LPSC process were investigated.

Result and Discussion

FE simulation-based casting design validation

After reverse engineering to determine the digital model of the part, remanufacturing by rapid LPSC begins with FE-simulation to identify hot spot positions, followed by the addition of the filling and risering systems according to design rules. For the present case study, two casting configuration are considered: horizontal (H) and vertical (V). **Fig. 3** shows the evolution of solid fraction during the cooling phase for both orientations. After thermal optimization, thermal-fluid flow simulations were performed to optimize process conditions (temperature and filling sequence) to avoid volume defects related to the filling and cooling phases such as misrun and shrinkage. All the thermal-physical properties for the alloy and mold , used in the FE simulation are summarized in **Table 2**.

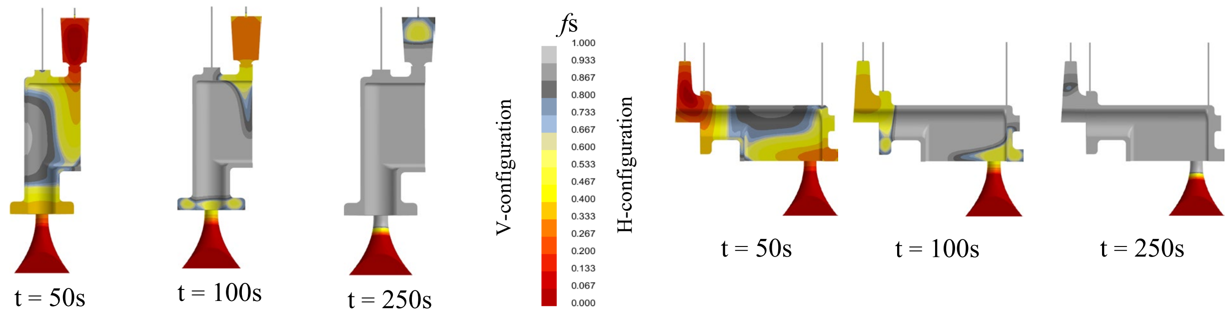

Fig. 3 FE-simulation of LPSC for V (left)- and H (right)- configuration

Table 2 Thermal-physical properties of the cast and 3DPSM

	T [°C]	Density [$kg.m^{-3}$]	Enthalpy [$kJ.kg^{-1}.°C^{-1}$]	Conductivity [$W.m^{-1}.°C^{-1}$]	Fraction solid	Viscosity [*cP*]
Alloy (AlSi7Mg03)	25	2675		154.2	1	-
	548 (T_{sol})	2565	542	175.0	1	-
	570	2522	564	125.0	0.49	1.746
	590	2511		101.2	0.35	1.607
	613 (T_{liq})	2473	1010	80.0	0	1.481
	720	2452	1246	80.0	0	1.153
Sand mold (Furan resin-bonded silica)	20	1590	670	0.71	-	-
	300		883	0.6		
	900		1006	0.73		

Surface deviation characteristics of the 3DPSM

In this work, all the mold parts for both H- and V-orientation are nested within the job box as shown in **Fig.4a**. Then the printing process was started until its completely finishing. It is important to note here that the printing resolution along X, Y and Z are defined as 0.11mm, 0.102 mm and 0.28 respectively. The Z resolution is defined indirectly since it is equal to twice the sand grain diameter. The X and Y resolutions are determined by the center-to-center spacing of adjacent inkjet nozzles within the printhead, which defines the minimum binder droplet deposition interval in the horizontal (in-plane) directions.

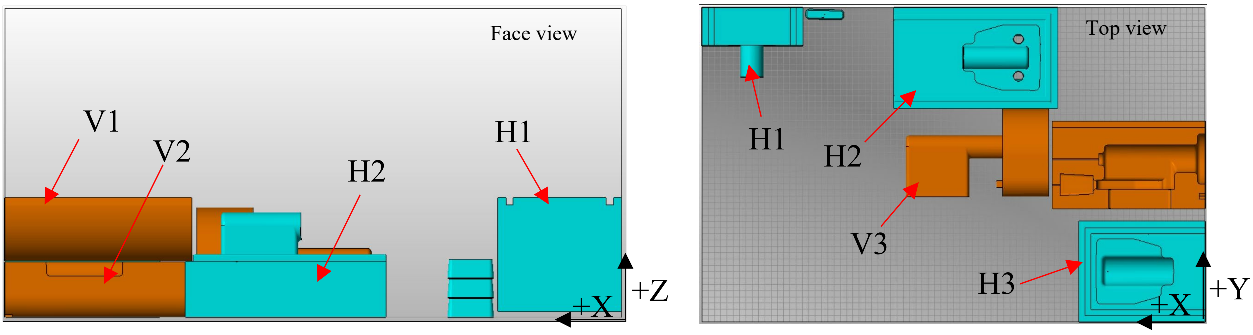

(a) Nesting of different H- and V- mold parts in the Jobbox prior to printing

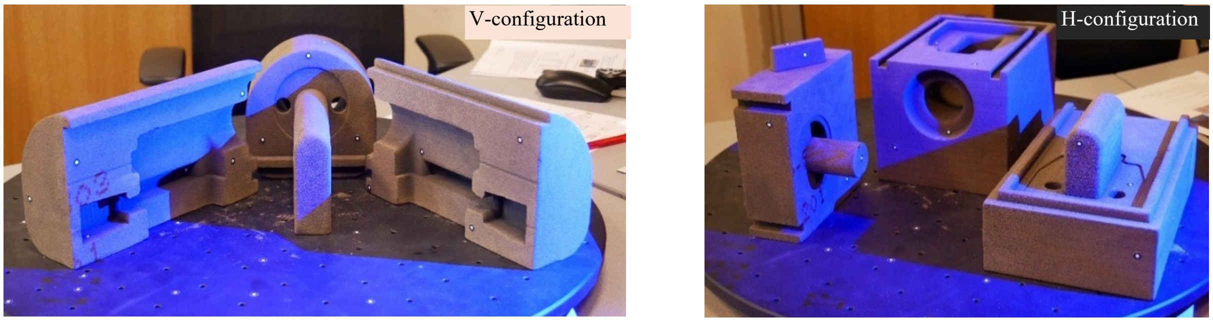

(b) 3D scanning of mold parts after 3D printing for both H- and V- configurations

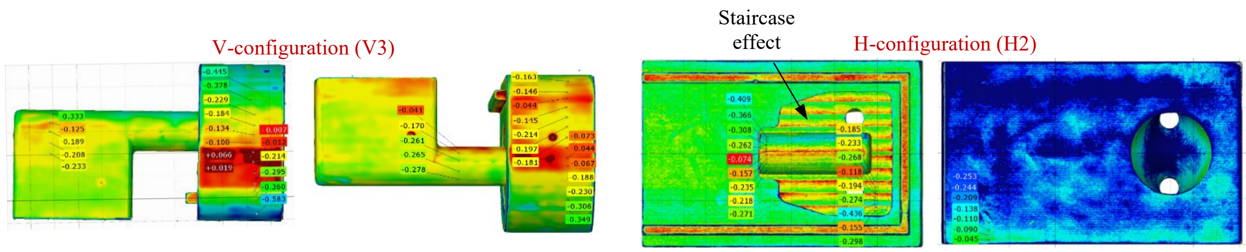

(c) 3D surface deviation of 3DPSM for both H- and V- configurations (one exemple per mold)

Fig. 4 Nesting of mold parts, 3D printing, and surface deviation inspection using 3D scanner

After printing, all parts were de-powdered and scanned with a 3D scanner to digitize their surfaces (**Fig. 4b**). The resulting 3D digital molds were compared to the original CAD models to assess dimensional deviations under the studied conditions. **Fig. 4c** shows an example of the 3D surface deviation map for mold parts V3 and H2, where the surface deviation value can be positive or negative compared to the original CAD model. The deviations are color coded for clarity with red indicating the upper limit of deviation, and blue representing the lower bound. For V3, printing accuracy decreases as angles increase in curved regions, a trend also confirmed by H2. Additionally, the top surfaces defining the cavities exhibit banding with deviations of approximately -0.1 to -0.4 mm, known as the staircase effect. Due to the resolution limits of sand grains, highly accurate angled or curved surfaces, especially at small angles relative to the horizontal plane (OXY), cannot be achieved. To estimate the average surface deviation caused by the printing process, a quantitative analysis was conducted on the scan data of all 3DPSM parts. **Fig. 5a** shows the legend associated with each scanned mold, where the maximum and minimum limits are defined using a $\pm 3\sigma$ criterion.

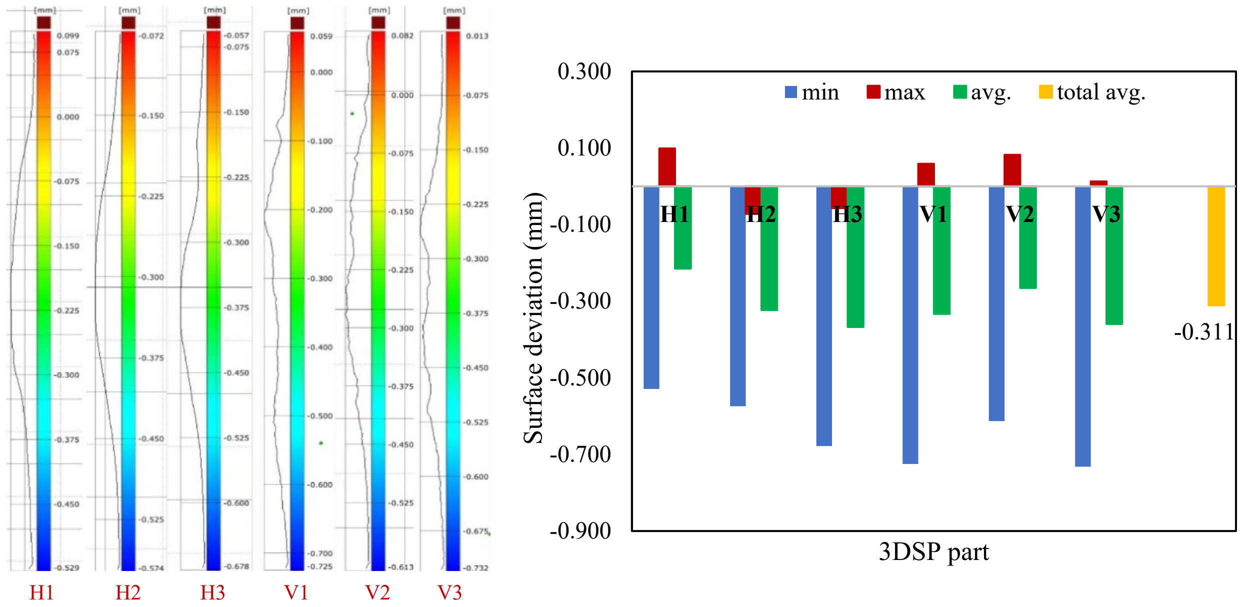

(a) 3σ surface deviation curves (mm) (b) Minimum, maximum, and average deviation values (mm)

Fig. 5 Dimensional deviation metrics on the 3DPSM parts compared to their CAD reference

Fig. 5a also shows the dispersal of the point cloud, which forms the generated mesh from the 3D scan, within this 3σ range. According to the color scale, points (i.e., regions) shown in yellow mostly correspond to the highest dimensional accuracy, indicating minimal deviation magnitude. For further understanding, the point cloud distribution obtained from all 3D scanned mold parts was postprocessed, and the maximum, minimum, and average deviation values are shown in **Fig. 5b**. It is clear that the surface deviation is mostly negative, with an average value of -0.311 mm. This result indicates that the printed sand mold parts have dimensions smaller than their initial CAD models.

3D surface deviation analysis of remanufactured as-cast

After mold assembly and completion of the LPSC process, the as-cast parts from both configurations underwent knockout and trimming, followed by 3D scanning to evaluate surface deviations, as shown in **Fig. 6**. Similar surface topologies are observed on the cast components, notably the staircase effect, which reflects the geometry of the mold surfaces. The measured surface deviations range from approximately -1.034 mm to +0.941 mm for the H configuration and from -0.931 mm to +0.837 mm for the V configuration. Regions shown in green indicate deviations close to zero. The red regions observed in the H configuration, corresponding to deviations exceeding +0.9 mm near the internal core surface, are likely due to core shift during mold assembly or the influence of molten metal flow within the mold cavity.

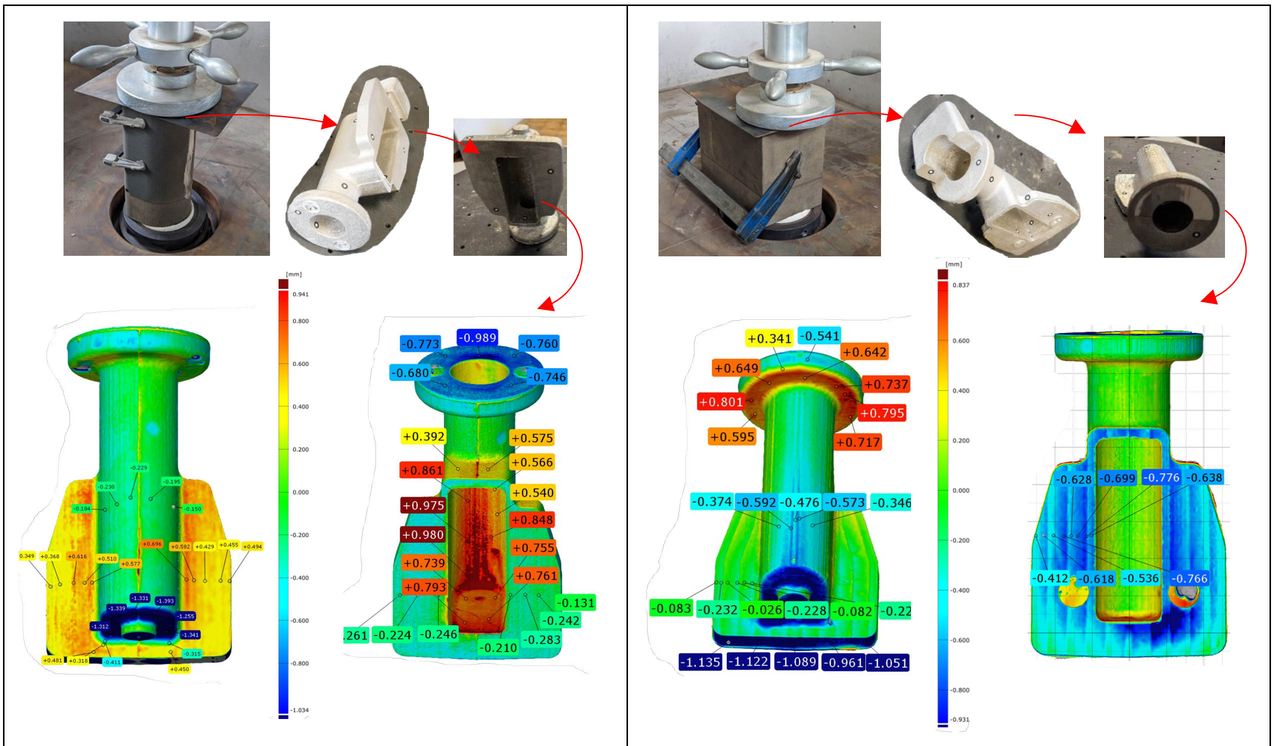

(a) H-configuration (b) V-configuration

Fig. 6 Castings from the LPSC process to 3D scan for both H- and V- configurations

To better understand the effect of the surface deviation on dimensional accuracy, a simplification method is followed in this work. The six characteristic cast dimensions presented in **Fig. 7** were calculated based on the 3D scanned casts and then compared to the initial CAD model to access the total dimensional deviation of the rapid LPSC process. **Fig.7a** shows an example of the followed procedure performed using Zeiss inspect® on the basis of the casting point cloud to find the value of the cylinder diameter. In this study , different fitting algorithms, such as *Gaussian*, *Chebytshev* and *Point median* were applied for each cylinder, surface, etc. to find the best fitted geometry.

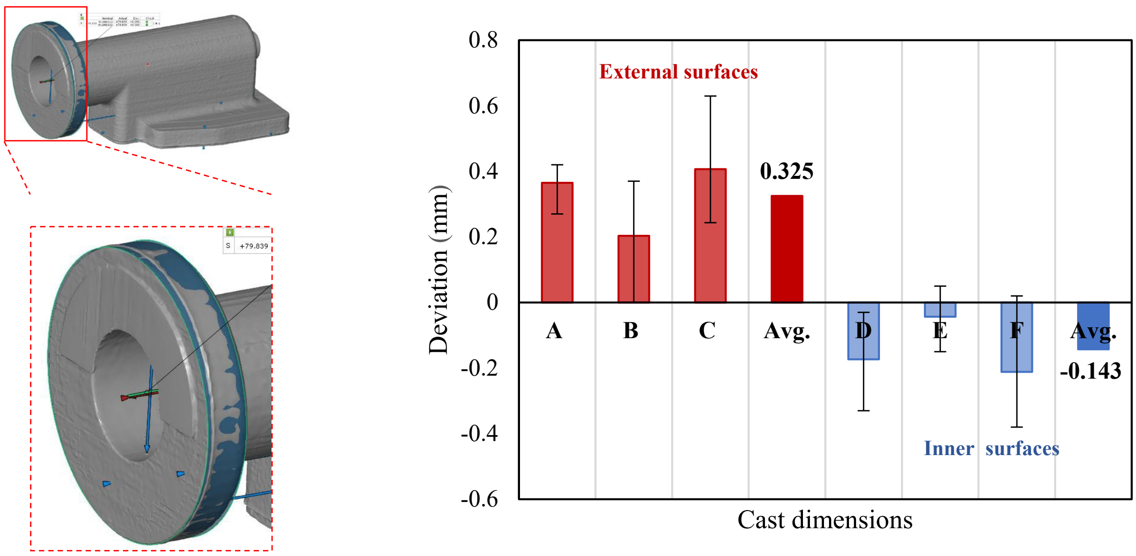

(a) Determination of cylinder nominal diameter "B"

(b) Dimensional deviation

Fig. 7. Dimensional deviation procedure performed on the characteristic casting dimensions

Fig. 7b shows the average dimensional deviation for both H and V casting orientations. The overall casting dimensions are very close to the target CAD dimensions. The average dimensional deviation does not exceed +0.41 mm and -0.21 mm for the C and F dimensions, respectively. **Fig. 7b** also shows that the deviation is mainly positive for the external casting surface, with an average value of 0.325 mm (i.e., twice the grain sand diameter), and negative for the inner surface, with an average value of -0.143mm (i.e., the grain sand diameter). The positive deviation in the external cast dimensions can be explained by the negative surface deviation of the printed mold parts. However, its negative deviations are mainly attributed to the mold constraint on casting shrinkage during the cooling phase [20].

Conclusion

This study demonstrates that rapid LPSC, combined with reverse engineering, 3D printing, and FE-based process optimization, can produce castings with high dimensional accuracy. Surface deviations in 3DPSM, primarily attributed to printing resolution determined by sand grain size, result in a negative surface deviation with an average value of -0.311 mm compared to the original CAD model. A simplification method was used to evaluate the dimensional accuracy of rapid LPSC castings by comparing six characteristic dimensions from 3D scanned parts to the original CAD model. Various fitting algorithms, including Gaussian, Chebyshev, and point-median methods, were used to determine the best-fit geometry. The results show that overall casting dimensions closely match the CAD model, with average deviations ranging from -0.21 mm to +0.41 mm. External surfaces exhibited slight positive deviations (approximately 0.325 mm) while internal surfaces showed minor negative deviations (approximately -0.143 mm) primarily caused by shrinkage constraints during cooling. The findings confirm that using the rapid LPSC process for manufacturing one-off replacement components can effectively minimize defects and ensure castings closely match the CAD design.

Furthermore, the proposed dimensional assessment methodology provides a practical means to evaluate the overall impact of the rapid LPSC process on part accuracy. Given the complex and varied sources of dimensional deviation, this approach can be extended to develop new mold design guidelines that consider not only literature-based expansion coefficients but also the cumulative effects of all process steps, thereby improving dimensional accuracy.

References

[1] B. Debnath, Z. Pourfarash, B. Ghorpade, S. Raman, Integrating Reverse Engineering for Digital Model Reconstruction and Remanufacturing of Mechanical Components: A Systematic Review, Metrology 5 (2025) 66. https://doi.org/10.3390/metrology5040066.

[2] A. Ktari, M.E. Mansori, Towards remanufacturing of failed parts through rapid low-pressure sand-casting (LPSC) process, Int J Adv Manuf Technol 139 (2025) 2569–2588. https://doi.org/10.1007/s00170-025-16049-x.

[3] G.-C. Vosniakos, S. Michael, A. Vasileiou, Digital Manufacturing Process Chain for One-Off Replacement Parts: A Precision Casting Case Study, JMMP 1 (2017) 17. https://doi.org/10.3390/jmmp1020017.

[4] A. Ktari, M. El Mansori, On the improvement of castings quality in hybrid low-pressure sand-casting (LPSC) process in a fully integrated CAE environment, Int J Adv Manuf Technol 127 (2023) 2309–2326. https://doi.org/10.1007/s00170-023-11663-z.

[5] İ. Aslan, A. Can, Effects of printing parameters on the mechanical properties of sand molds produced by a novel binder jetting 3D printer, Prog Addit Manuf 10 (2025) 2939–2950. https://doi.org/10.1007/s40964-024-00795-7.

[6] D. Snelling, H. Blount, C. Forman, K. Ramsburg, A. Wentzel, C. Williams, A. Druschitz, The effects of 3D printed molds on metal castings, (2013) 827–845.

[7] N. Coniglio, T. Sivarupan, M. El Mansori, Investigation of process parameter effect on anisotropic properties of 3D printed sand molds, Int J Adv Manuf Technol 94 (2018) 2175–2185. https://doi.org/10.1007/s00170-017-0861-5.

[8] M. Bedel, A. Fabre, N. Coniglio, Defining the printing direction impact of additively manufactured sand molds on casting roughness, Journal of Manufacturing Processes 116 (2024) 329–340. https://doi.org/10.1016/j.jmapro.2024.02.068.

[9] A. Sanitas, N. Coniglio, M. Bedel, M. El Mansori, Investigating surface roughness of ZE41 magnesium alloy cast by low-pressure sand casting process, Int J Adv Manuf Technol 92 (2017) 1883–1891. https://doi.org/10.1007/s00170-017-0283-4.

[10] S.S. Gill, M. Kaplas, Efficacy of powder-based three-dimensional printing (3DP) technologies for rapid casting of light alloys, Int J Adv Manuf Technol 52 (2011) 53–64. https://doi.org/10.1007/s00170-010-2716-1.

[11] D. Brabazon, D. Kennedy, M. Tyrell, Development of Technique for 3D Printed Mould Intricate Rapid Casting, (2010). https://doi.org/10.26153/TSW/15244.

[12] D. Dimitrov, W. Van Wijck, K. Schreve, N. De Beer, J. Meljer, An Investigation of the Capability Profile of the Three Dimensional Printing Process with an Emphasis on the Achievable Accuracy, CIRP Annals 52 (2003) 189–192. https://doi.org/10.1016/S0007-8506(07)60562-9.

[13] D. Martinez, C. Bate, G. Manogharan, Towards Functionally Graded Sand Molds for Metal Casting: Engineering Thermo-mechanical Properties Using 3D Sand Printing, JOM 72 (2020) 1340–1354. https://doi.org/10.1007/s11837-019-03975-x.

[14] H. Liu, T. Lei, F. Peng, Compensated printing and characterization of the droplet on the binder migration pattern during casting sand mold 3D printing, Journal of Manufacturing Processes 108 (2023) 114–125. https://doi.org/10.1016/j.jmapro.2023.10.073.

[15] T. Ollison, K. Berisso, Three-dimensional printing build variables that impact cylindricity, Journal of Industrial Technology (2010) 10.

[16] H. Khandelwal, B. Ravi, Effect of molding parameters on chemically bonded sand mold properties, Journal of Manufacturing Processes 22 (2016) 127–133. https://doi.org/10.1016/j.jmapro.2016.03.007.

[17] D. Galles, C. Beckermann, Prediction of distortions and pattern allowances during sand casting of a steel bracket, International Journal of Cast Metals Research 30 (2017) 133–147. https://doi.org/10.1080/13640461.2016.1262984.

[18] S. Ravi, J. Thiel, Increasing the Capabilities of Computer Process Modeling with Applied Programming Interface, Inter Metalcast 11 (2017) 101–115. https://doi.org/10.1007/s40962-016-0104-9.

[19] J.M. Walker, A. Prokop, C. Lynagh, B. Vuksanovich, B. Conner, K. Rogers, J. Thiel, E. MacDonald, Real-time process monitoring of core shifts during metal casting with wireless sensing and 3D sand printing, Additive Manufacturing 27 (2019) 54–60. https://doi.org/10.1016/j.addma.2019.02.018.

[20] H. Khandelwal, B. Ravi, Effect of varying part geometry and mold constraints on dimensional deviations of sand cast parts, Int J Interact Des Manuf 19 (2025) 4973–4986. https://doi.org/10.1007/s12008-024-02118-0.